Supplementary Information

Three-Dimensional Splitting Microfluidics

Yongping Chen,[ab] *Wei Gao,*[b] *Chengbin Zhang*[b] *and Yuanjin Zhao*[c]

[a]School of Environmental Science and Engineering,

Suzhou University of Science and Technology, Suzhou 215009, P. R. China

[b]Key Laboratory of Energy Thermal Conversion and Control of Ministry of Education,

School of Energy and Environment, Southeast University, Nanjing 210096, P. R. China

[c]State Key Laboratory of Bioelectronics, School of Biological Science and Medical

Engineering, Southeast University, Nanjing 210096, P. R. China

Experimental Section.

   Materials. The surfactant poly (vinyl alcohol) (PVA), 0.65CS polydimethylsiloxane, ethoxylated trimethylolpropane triacrylate (ETPTA) resin, hydroplethilic reagent 3-aminopropyltriethoxysilane (3-APTES), and hydroplethobic reagent octadecyltrichlorosilane (OTS) were all purchased from Sigma-Aldrich Co. The absolute ethyl alcohol and acetone were from Sinopharm Chemical Reagent Co. To achieve better mixing, the 3-APTES with volume fraction of 5% was added to absolute ethyl alcohol, and OTS with a volume fraction of 5% was added to acetylacetone. Deionized water was used in all experiments.

   Microfluidics. The theta(θ)-shaped capillary, three-bore capillary, compression capillary, fixed capillary and square capillary were obtained from World Precision Instruments, Inc. The inner and outer diameters of the three-bore capillary were 750 μm and 1 mm, respectively. The inner and outer diameters of the compression capillary were 300 μm and 580 μm, respectively. The inner and outer diameters of the fixed capillary were 580 μm and 1 mm,

respectively. The square capillary with an inner diameter of 1.05 mm was obtained from VitroCom, Inc. The droplet maker was assembled using a glass capillary; the resulting droplet maker produced single emulsions and double emulsions. The splitting capillaries, including the θ-shaped capillary and three-bore capillary, were tapered using a laboratory portable Bunsen burner (Honest MicroTorch). The Bunsen burner was set to its median thermal power and after a heating period of 3 s, the splitting capillaries were stretched by hand to reach a diameter of approximately 580 μm at the orifice. For the treatment of the capillary, they were immersed in the 5% octadecyltrichlorosilane (OTS) acetylacetone solution to make the capillary hydroplethobic and were immersed in 5% 3-aminopropyltriethoxysilane (3-APTES) absolute ethyl alcohol solution to make the capillary hydroplethilic for 8 hours at room temperature. Subsequently, the solution was blown out. Next, the compression capillary and splitting capillaries were inserted into a fixed capillary inside a square capillary. The connectors of the assembled capillaries were then sealed with dispensing needles by the use of transparent epoxy resin (Devcon 5 Minute Epoxy) where necessary.

Emulsification. The microfluidic device was used to split oil-in-water (O/W) single emulsions for obtaining monodisperse single emulsions and oil-in-oil-in-water (O/O/W) double emulsions for obtaining monodisperse double emulsions. For single emulsions, the inner phase (ethoxylated trimethylolpropane triacrylate (ETPTA) resin) and the outer phase (water with 2% poly (vinyl alcohol) (PVA) as a surfactant) flowed in the same direction via the injection capillaries in an appropriate arrangement, as required. For double emulsions, the inner phase (0.65CS polydimethylsiloxane), middle phase (ethoxylated trimethylolpropane triacrylate (ETPTA) resin), and outer phase (water with 2% poly (vinyl alcohol) (PVA) as a surfactant) flowed in the same direction via the injection capillaries in an appropriate arrangement, as required. Each fluid was pumped using a syringe pump (Harvard PHD 2000 Series) and was linked through a polyethylene tube (Scientific Commodities Inc., with inner and outer diameters of 0.86 mm and 1.32 mm, respectively) with a glass syringe (SGE

Analytical Science). The produced daughter droplets are collected in a half-filled open glass petri dish with diameter of 51.4mm and height of 15mm, still having good sphericity. The processes of splitting single and double emulsions into two or three portions were observed in real time using an inverted microscope (AE2000, Motic) and were recorded by a charged coupled device (CCD, S-PRI F1, AOS Technologies AG). The optical images of the emulsions were observed using a stereomicroscope (NOVEL NTB-3A, Ningbo Yongxin Optics Co., Ltd, China) and were captured by a CCD (Media Cybernetics Evolution MP 5.0 RTV). The radius of single emulsions and the inner radius and outer radius of the double emulsions were all measured using Image-Pro Plus 7.0 software.

Hydraulic resistances analysis. To fully understand the splitting function of the current 3D microfluidic device, we performed a theoretical analysis of the dynamics of emulsion droplet flow in the microfluidics device. The dynamics can be understood through the microfluidic analog of an electrical current splitting device in which the flow rate of the nth splitting channel, q_n, is analogous to a branch current, and the pressure head is analogous to an electric voltage. In microfluidics, the pressure drop can be described as

$$\Delta P = RV \tag{1}$$

where R is the total hydraulic resistance of microchannel and V is the flow velocity. Because the split capillary comprises N 3D symmetrical capillary collection microchannels, the whole flow resistance R of the split capillary is expressed as

$$\frac{1}{R} = \sum_{n=1}^{N} R_n \tag{2}$$

where R_n is the flow resistance of the nth microchannel. Accordingly, before the first split of droplet, only the single phase continuous fluid flows through the split capillary, which produces total hydraulic resistances as

$$R_{n0} = R_{n0}^{f} + R_{n0}^{m} \tag{3}$$

where R_{n0}^{f} is the friction hydraulic resistance and R_{n0}^{m} is the local hydraulic resistance due to the gradual conical diverging inlet of the split capillary. Note that, in the current work, due to the small diverging angle (8.2° ~ 19.4°) and length (less than 11.3% of the total length of the split capillary), R_{n0}^{m} can be neglected with respect to the R_{n0}.[1] Therefore, the hydraulic resistances in each split capillary can be described as[2]

$$R_{n0} = R_{n0}^{f} = \frac{4\pi^2\mu}{\left(\pi^2\text{-}8\right)r_s^2}L \quad \text{for semicircular split capillaries in θ-shaped split device} \quad (4)$$

$$R_{n0} = R_{n0}^{f} = \frac{8\mu}{r_c^2}L \quad \text{for circular split capillaries in three-bores split device} \quad (5)$$

where r_s and r_c is the radius of semicircular and circular, respectively, μ is the viscosity of the liquid, and L is the total length of the split capillary. After the first split, the droplet flow dynamics in a microchannel is governed by a visco-capillary regime,[3] and its whole hydraulic resistance in n^{th} microchannel is expressed as

$$R_n = R_n^s + R_n^c + R_n^v + R_n^m \quad (6)$$

where R_n^s is the total spacing resistance between two droplets, R_n^c is the total capillary resistance of all droplets containing the receding and advancing interfaces, R_n^v is the total resistance due to viscous dissipation occurring in the droplets bodies, and R_n^m is the local resistance due to the gradual conical diverging geometry of the split capillary. Similar to R_{n0}^{m}, R_n^m can also be neglected with respect to R_n. Therefore, R_n^s in Equation 6 can be given by

$$R_n^s = \frac{4\pi^2\mu}{\left(\pi^2\text{-}8\right)r_s^2}\left(L - L_d\right) \quad \text{for semicircular split capillaries in θ-shaped split device} \quad (7)$$

$$R_n^s = \frac{8\mu}{r_c^2}\left(L - L_d\right) \quad \text{for circular split capillaries in three-bores split device} \quad (8)$$

where L_d is sum of lengths of all droplets in the split capillary. According to the related research,[4-11] R_n^c in Equation 6 scales as σ/r and $Ca^{2/3}$, where σ is the surface tension and capillary number $Ca = (\mu V)/\sigma$. Thus, R_n^c can be described as

$$R_n^c = \frac{m\beta\mu Ca^{-1/3}}{r} \qquad (9)$$

where m is the number of the droplets in the split capillary, β is the dimensionless parameter dependent on the radius r (r_s or r_c). In addition, R_n^v in Equation 6 can be estimated using Poiseuille's law:[12]

$$R_n^v = \alpha(D_h)\mu L_b \qquad (10)$$

where α is a dimensional coefficient, related to the hydraulic diameter[13-15] and L_b is sum of lengths of all droplets bodies except two tips, and D_h is the hydraulic diameter of the split capillary calculated by

$$D_h = \frac{2r_s}{1+2/\pi} \quad \text{for semicircular split capillaries in θ-shaped split device} \qquad (11)$$

$$D_h = 2r_c \quad \text{for circular split capillaries in three-bores split device} \qquad (12)$$

It is important to note that the ratio among hydraulic resistances in subchannels is mainly inversely proportional to that among volume flow rates (average flow velocity) there, which determines the ratio among volumes of daughter droplets in subchannels.[16] Therefore, according to Equations 4 and 5, the uniform structure among the split capillaries in the current microfluidic device can produce uniform hydraulic resistance among the split capillaries, which generates the first uniform split, and thus produces equal-size droplet in each split capillary. After the first split, it can be seen for Equations 6 ~ 12 that the whole resistance of every split capillary is related to the viscosity of the continuous liquid, the length of the produced droplets, and the geometry of the split capillary (i.e. the hydraulic diameter and the

length). Therefore, in view of the uniform geometry of split capillary and the first uniform split, our microfluidic device can produce uniform split of emulsions subsequently.

Notes and references

1 F. M. White, *Fluid mechanics*, New York: McGraw-Hill, 2009.

2 C. J. Morris and F. K. Forster, *Exp. Fluids*, 2004, **36**, 928-937.

3 C. P. Ody, C. N. Baroud and E. De Langre, *J. Colloid Interface Sci.*, 2007, **308**, 231-238.

4 F. P. Bretherton, *J. Fluid Mech.*, 1961, **10**, 166-188.

5 H. Wong, C. J. Radke and S. Morris, *J. Fluid Mech.*, 1995, **292**, 71-94.

6 H. Wong, C. J. Radke and S. Morris, *J. Fluid Mech.*, 1995, **292**, 95.

7 H. Kim, D. Luo, D. Link, D. A. Weitz, M. Marquez and Z. Cheng, *Appl. Phys. Lett.*, 2007, **91**, 133106.

8 L. Salkin, L. Courbin and P. Panizza, *Phys. Rev. E*, 2012, **86**, 036317.

9 A. Schmit, L. Salkin, L. Courbin and P. Panizza, *Soft matter*, 2015, **11**, 2454-2460.

10 M. J. Fuerstman, A. Lai, M. E.Thurlow, S. S. Shevkoplyas, H. A. Stone and G. M. Whitesides, *Lab Chip*, 2007, **7**, 1479-1489.

11 A. Carlson, M. Do-Quang, and G. Amberg, *Int. J. of Multiph. Flow*, 2010, **36**, 397-405.

12 F. M. White and I. Corfield, *Viscous fluid flow*, New York: McGraw-Hill, 2006.

13 H. A. Stone, A. D. Stroock and A. Ajdari, *Annu. Rev. Fluid Mech.*, 2004, **36**, 381-411.

14 R. K. Shah and A. L. London, *Laminar flow forced convection in ducts: a source book for compact heat exchanger analytical data*, Academic press, 2014.

15 H. Bruus, *Theoretical Microfluidics*, Oxford University Press, 2008.

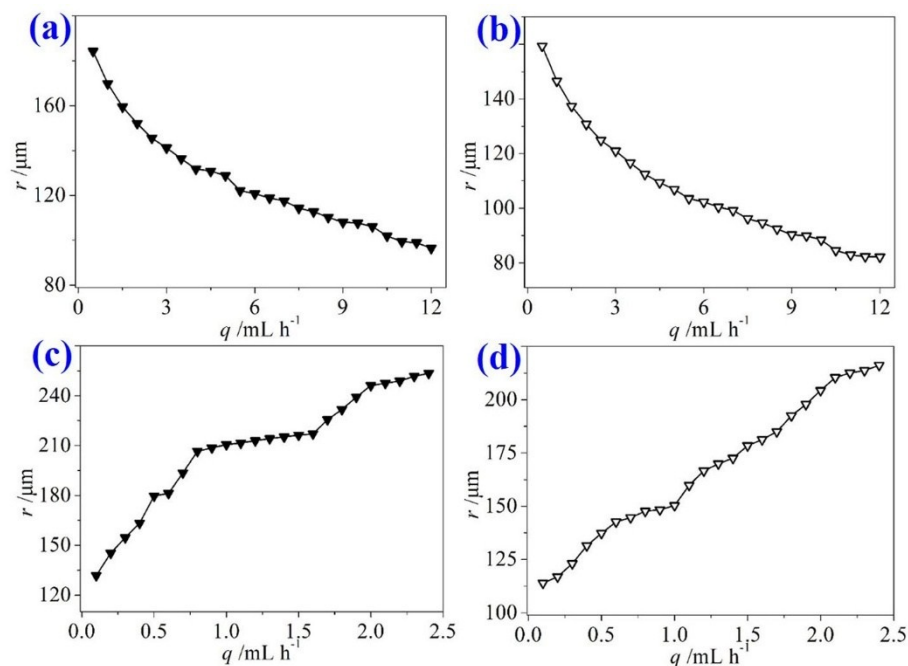16 T. Nisisako, T. Ando and T. Hatsuzawa, *Lab Chip*, 2012, **12**, 3426-3435.

Figure S1. Relationships between the flow rate and the single emulsion radius after splitting. (a, b) The radius of single emulsions split into (a) two and (b) three portions with a constant inner phase flow rate of 0.1 mL h^{-1} and a metabol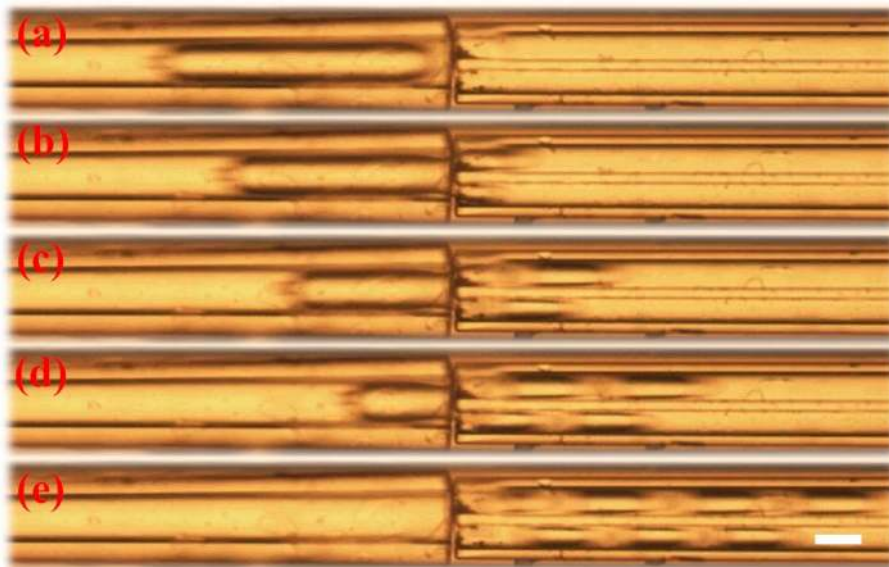ic outer phase flow rate ranging from 0.1 to 12 mL h^{-1}. (c, d) The radius of splitting single emulsions into (c) two and (d) three portions with a constant outer phase flow rate of 4 mL h^{-1} and a metabolic inner phase flow rate ranging from 0.1 to 2.4 mL h^{-1}.

Figure S2. Real-time images at an interval of 0.02 s of the microfluidic process of splitting single emulsions. The corresponding flow rates of the inner (outer) phases are: 5 mL h^{-1} (12 mL h^{-1}). The scale bar is 300 μm, $Ca = 0.021$.
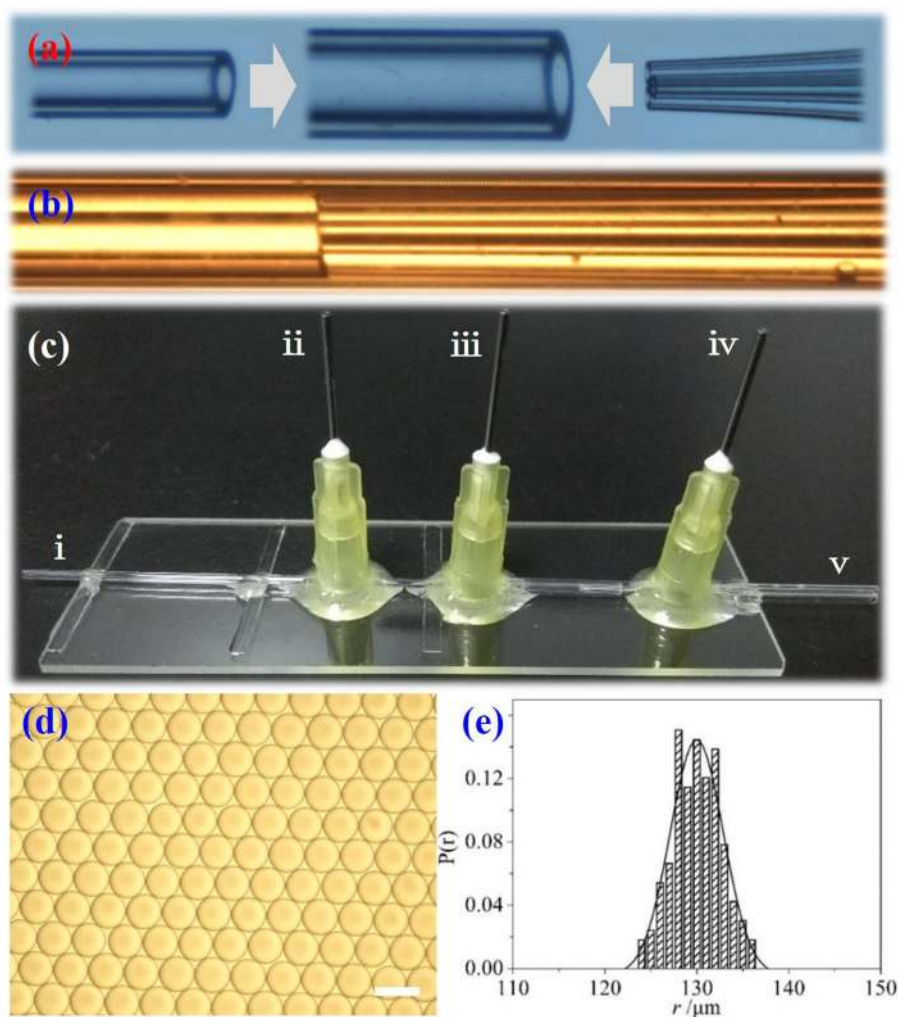
Figure S3. The microfluidic device with a three-bore capillary for splitting single emulsions into three portions. (a) an assembly process diagram of the compression capillary, the tapered three-bore capillary and the fixed capillary (this tapered capillary is an example and not exactly what we used in our experiments); (b, c) the digital microscope photographs of the assembled capillary microfluidic device, where i–v are the inner, outer, compression, fixed, and three-bore channels, respectively; (d) images of single emulsions split into three portions; (e) the corresponding radius distribution of single emulsions with flow rates of the inner phase and outer phase 0.3 mL h^{-1} and 4 mL h^{-1}, respectively. The scale bar is 300 μm.
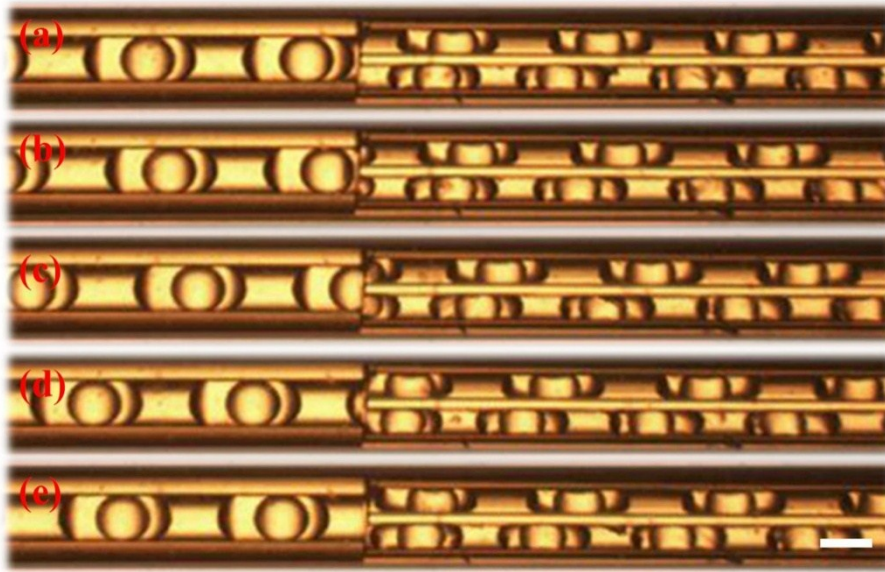
Figure S4. Real-time images at an interval of 0.1 s of splitting double emulsions into two portions. The scale bar is 300 μm.
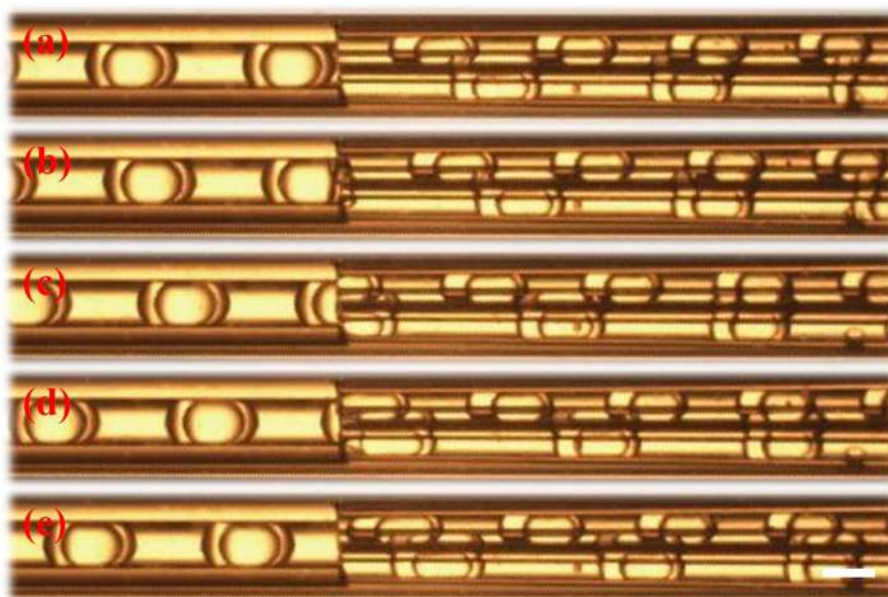
Figure S5. Real-time images at an interval of 0.12 s of the microfluidic process of splitting double emulsions into three portions. The scale bar is 300 μm.
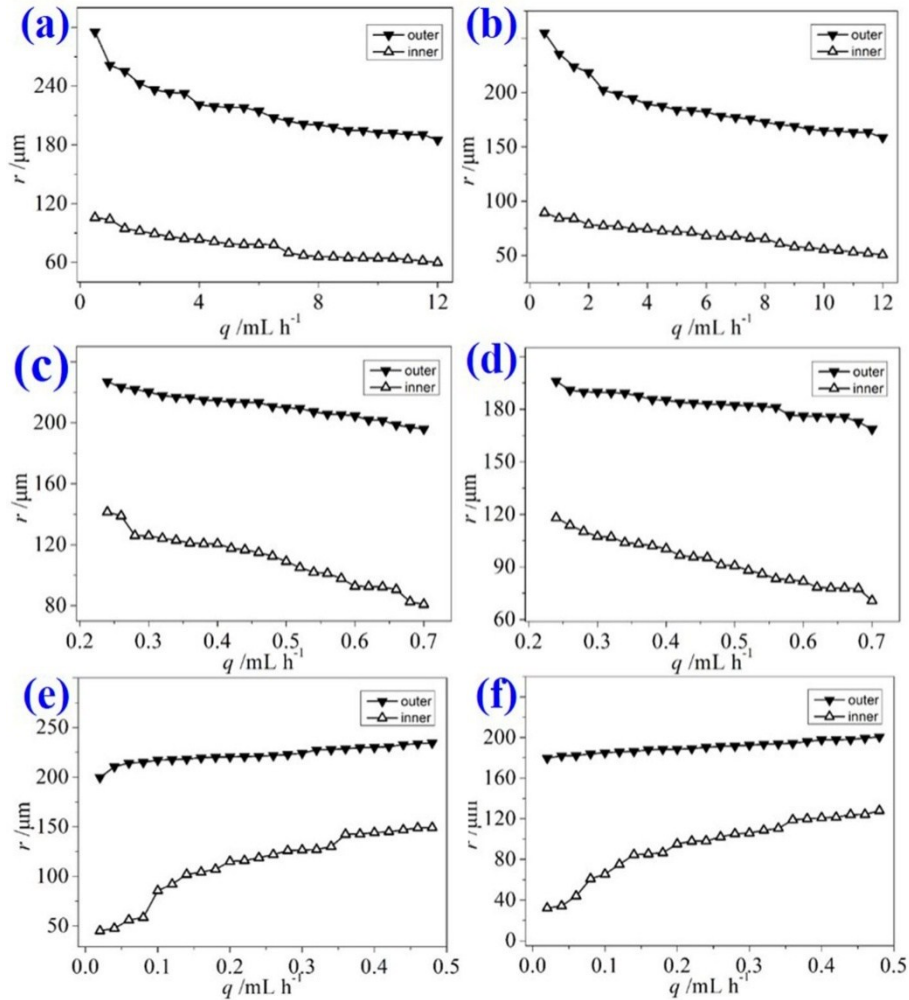
Figure S6. Relationships between the flow rate and the radius of the double emulsions after splitting. (a, b) The inner and outer radius of splitting double emulsions into (a) two and (b) three portions with constant inner and middle phase flow rates of 0.1 mL h^{-1} and 1 mL h^{-1}, respectively, and metabolic outer phase flow rates ranging from 0.5 to 12 mL h^{-1}. (c, d) The inner and outer radius of splitting double emulsions into (c) two and (d) three portions with constant inner and outer phase flow rates of 0.1 mL h^{-1} and 4 mL h^{-1}, respectively, and metabolic middle phase flow rates ranging from 0.24 to 0.7 mL h^{-1}. (e, f) The inner and outer radius of splitting double emulsions into (e) two and (f) three portions with constant inner and outer phase flow rates of 1 mL h^{-1} and 4 mL h^{-1}, respectively, and metabolic inner phase flow rates ranging from 0.02 to 0.48 mL h^{-1}.